Inverse Problems **24** (2008) 025023 (15pp) doi:10.1088/0266-5611/24/2/025023

A Rao–Blackwellized particle filter for magnetoencephalography

C Campi[1], A Pascarella[1], A Sorrentino[2] and M Piana[3]

[1] Dipartimento di Matematica, Università di Genova, via Dodecaneso 35, 16146 Genova, Italy
[2] CNR-INFM LAMIA, via Dodecaneso 33, 16146 Genova, Italy
[3] Dipartimento di Informatica, Università di Verona, Ca` Vignal 2, Strada le Grazie 15, 37134 Verona, Italy

E-mail: michele.piana@univr.it

Received 17 July 2007, in final form 8 February 2008
Published 11 March 2008
Online at stacks.iop.org/IP/24/025023

Abstract
A Rao–Blackwellized particle filter for the tracking of neural sources from biomagnetic data is described. A comparison with a sampling importance resampling particle filter performed in the case of both simulated and real data shows that the use of Rao–Blackwellization is highly recommended since it produces more accurate reconstructions within a lower computational effort.

1. Introduction

Magnetoencephalography (MEG) [8] is a powerful tool for brain functional studies which measures non-invasively the magnetic field outside the head with outstanding temporal resolution (about 1 ms). The neurophysiological aim of MEG experiments is to recover the dynamical behavior of the neural electrical currents which are responsible for the measured field [9]. From a mathematical viewpoint the formation of the biomagnetic signal induced by spontaneous or stimulus-induced current density distributions is described by the Biot–Savart equation [14], which is a linear integral equation of the first kind. The Biot–Savart linear operator mapping the current density onto the magnetic field is compact [2] and has a non-trivial kernel [11]. Therefore the problem of restoring the current density from measurements of the magnetic field is a linear ill-posed inverse problem. This problem can be addressed, for example, by beamforming procedures which apply linear spatial filters on the MEG series [15, 21]; or by standard regularization methods, whereby a numerically stable current density distribution is determined by solving a Tikhonov-like minimum problem [7, 20]. Beamformers are particularly useful in extracting on-going, even notably weak brain activity in a certain location in the brain, but have difficulties in reconstructing temporally correlated sources. The main advantages of Tikhonov-like methods are a great generality of the applicability conditions and, in the case of L^2 penalty terms, a notable computational effectiveness. However regularized reconstructions often present a significant drawback: the support of

the restored distributions is in fact typically too widespread with respect to physiology and even the sparsity enhancement guaranteed by the use of L^1 penalty terms in the Tikhonov functional results insufficient [20].

Physiological information on the current density distribution can be easily coded by using parametric models for representing the neural sources: the most utilized one in the MEG community consists in approximating the neural current distribution with a small set of point-like currents, named *current dipoles* [8]. This approach leads to a nonlinear parameter identification problem which can be addressed by optimization methods like Multiple SIgnal Classification (MUSIC) [12] or by Bayesian filtering approaches [16]. In the Bayesian setting [10], both the data and the unknown are modeled as random variables and the goal is to construct the posterior probability density function for the unknown variable, conditioned on the realization of the data random variable. The key equation of this framework, which allows constructing the posterior density, is Bayes theorem where prior information are combined with the information coming from the data. Bayesian filtering is a framework for facing dynamical problems, where the unknown and the data form two stochastic processes and the transition kernel of the unknown stochastic process is assumed to be known. For linear models and Gaussian densities, Bayesian filtering reduces to the computation of the Kalman filter [10], where the mean value and the covariance matrix are sequentially updated in time. However, more generally, the numerical implementation of Bayesian filtering requires the use of numerical integration techniques provided by the so-called *particle filters* [1] which are essentially a class of sequential Monte Carlo methods where the support points, called particles, evolve with time according to the transition kernel of the unknown process.

The use of particle filters for the solution of the MEG inverse problem has been introduced in [16] in the case of simulated data while in [17] it has been generalized to a more realistic framework and applied to experimental time series recorded during auditory external stimulation and in [13] it has been compared to other reconstruction algorithms. However, in these implementations, the application of particle filtering to complex neurophysiological experiments is limited by a notable computational effort which rapidly becomes unaffordable when many time points must be analyzed and several simultaneous point sources are evoked by the stimulus. The aim of the present paper is to introduce a mathematical procedure which notably reduces this numerical heaviness by exploiting a specific mathematical feature of the MEG inverse problem. In fact, the parametric model which describes the spatio-temporal behavior of the biomagnetic field is nonlinear with respect to the position of the point sources but linear with respect to their amplitude. In this situation a rather straightforward analysis of variance shows that a particle filter algorithm computing the posterior probability density function associated with the source position is much more accurate than the particle filter computing the probability density function associated with the whole current density. On the basis of this result, we apply a computational procedure, named Rao–Blackwellization [3], where a particle filter approximates the probability density function associated with the source position while mean and variance of the source amplitude are optimally determined by means of set of Kalman filters. The result is a more efficient code, which reconstructs the source dipoles more rapidly than a standard particle filter, with a better accuracy and a better use of the computational resources at disposal.

The plan of the paper is as follows. In section 2 we briefly describe the mathematical model for the MEG inverse problem. Section 3 introduces the Bayesian filtering approach together with standard particle and Kalman filters. In section 4 the Rao–Blackwell method is discussed for the MEG inverse problem and in section 5 applied to both simulated and real biomagnetic time series. Finally, section 6 contains our conclusion and a brief description of the main work-in-progress.

2. The MEG inverse problem

In the quasi-static approximation [14], a current density $\mathbf{j}(\mathbf{r})$ inside a volume Ω produces a magnetic field given by the Biot–Savart equation

$$\mathbf{b}(\mathbf{r}, t) = \frac{\mu_0}{4\pi} \int_\Omega \mathbf{j}(\mathbf{r}', t) \times \frac{\mathbf{r} - \mathbf{r}'}{|\mathbf{r} - \mathbf{r}'|^3} \, \mathrm{d}\mathbf{r}', \tag{1}$$

where μ_0 is the magnetic permittivity of vacuum and can be considered constant in the volume Ω too. When equation (1) refers to the generation of magnetic fields from the brain, the current density $\mathbf{j}$ is usually split in two terms: the 'primary' current $\mathbf{j}^p$, of neural origin, and the 'volume' current $\mathbf{j}^v = \sigma \mathbf{E}$, arising because of the nonzero conductivity of the human brain. In the MEG inverse problem, one is interested in recovering $\mathbf{j}^p$ from the measured field produced by both $\mathbf{j}^p$ and $\mathbf{j}^v$. In general, the presence of volume currents imply that the forward computation must be performed by means of numerical approximations such as boundary element or finite element methods. In order to simplify the computation, one can assume that:

- the primary current is a sum of N_d point-like currents, named 'current dipoles'

$$\mathbf{j}^p(\mathbf{r}, t) = \sum_{i=1}^{N_d} \mathbf{q}_i(t) \delta(\mathbf{r} - \mathbf{r}_i(t)), \tag{2}$$

  each one parameterized by six parameters at a fixed time point: three parameters for the position $\mathbf{r}_i$ and three for the dipole moment $\mathbf{q}_i$;
- the head volume Ω is a sphere of constant conductivity σ (whose explicit value is not necessary for the computation). This approximation leads to reliable results for activations not in the frontal lobe, i.e. in cortical regions where the brain is closer to a spherical shape. This assumption can be relaxed if some boundary or finite element method is applied for solving equation (1) [6]. Anyway, what discussed in the following and, in particular, what is concerned with the particle and Rao–Blackwellized particle filtering methods still hold also in this more general setting.

Given the two previous assumptions, an analytic formula is available which accounts for the contribution of both the primary and the volume current ([14]),

$$\mathbf{b}(\mathbf{r}, t) = \sum_{i=1}^{N_d} \frac{\mu_0}{4\pi f_i^2(t)} (f_i(t)\mathbf{q}_i(t) \times \mathbf{r}_i(t) - \mathbf{q}_i(t) \times \mathbf{r}_i(t) \cdot \mathbf{r} \nabla f_i(t)) \tag{3}$$

with $f_i(t) = a_i(t)(r a_i(t) + r^2 - \mathbf{r}_i(t) \cdot \mathbf{r})$, $\mathbf{a}_i(t) = \mathbf{r} - \mathbf{r}_i(t)$, $a_i(t) = |\mathbf{a}_i(t)|$, $r = |\mathbf{r}|$.

Equation (3) defines the parameter identification problem we want to solve, i.e. to dynamically reconstruct $\mathbf{r}_i(t)$ and $\mathbf{q}_i(t)$ from measurements of $\mathbf{b}(\mathbf{r}, t)$. We observe that the problem is clearly nonlinear, as the dipole positions are among the unknowns; at the same time, the dependence of $\mathbf{b}$ on the dipole moments $\mathbf{q}_i$ is linear. In the following, we will denote by $\mathbf{b}_k$ the (noisy) spatial sampling of the magnetic field at time t_k, and by $\mathbf{j}_k$ (omitting the p superscript) the primary current at time t_k.

3. Bayesian filtering

In the Bayesian approach to inverse problems [10], all the quantities of interest are modeled as random vectors; here we briefly recall the basics of Bayesian filtering, which is a powerful framework for solving dynamical inverse problems. The time-varying unknown is modeled as a stochastic process, $\{X_k\}_{k=1}^T$, and the sequence $y_1, \ldots, y_T$ of measurements is considered as

a realization of the data stochastic process $\{Y_k\}_{k=1}^T$. We assume that the data and the unknown are related by the following model:

$$Y_k = G_k(X_k, N_k), \tag{4}$$

where the random variables N_k account for the presence of noise and G_k is a known, possibly nonlinear function of its arguments for each time step k. We further assume that the stochastic process $\{X_k\}_{k=1}^T$ evolves according to the following model:

$$X_{k+1} = F_k(X_k, \Delta X_k), \tag{5}$$

where ΔX_k is the process noise and F_k is a known, possibly nonlinear function of its arguments for each time step k.

The natural framework for applying Bayesian filtering is that of Markov processes. The Markovian nature of the two stochastic processes $\{X_k\}_{k=1}^T$ and $\{Y_k\}_{k=1}^T$ is synthesized by the equations

$$\pi(x_k|x_{1:k-1}) = \pi(x_k|x_{k-1}), \tag{6}$$

$$\pi(y_k|x_{1:k}) = \pi(y_k|x_k) \tag{7}$$

and

$$\pi(x_{k+1}|x_k, y_{1:k}) = \pi(x_{k+1}|x_k), \tag{8}$$

where we use the notation $x_{1:k} = \{x_1, x_2, \ldots, x_k\}$; equation (6) states that the process X is a (first-order) Markov process, equation (7) states that the process Y is a Markov process with respect to the history of X and equation (8) states that the unknown does not depend on the measurements, if conditioned on its own history. If equations (6)–(8) are satisfied, Bayesian filtering provides optimal solutions for the model (4)–(5). We point out that the dynamics and interplay of cortical signals are certainly more complicated and cannot be reduced to first-order Markov processes (the investigation of more realistic and sophisticated models for the dynamics of cortical signals is still an open issue of great neuroscientific significance which is far from the aims of the present paper). However Bayesian filtering provides optimal solutions even in the case of higher order Markov processes [16] and, for more complicated models, it gives reliable approximations to the model equations.

The Bayesian filtering algorithm is the sequential application of the two following equations:

$$\pi(x_k|y_{1:k}) = \frac{\pi(y_k|x_k)\pi(x_k|y_{1:k-1})}{\pi(y_k|y_{1:k-1})} \tag{9}$$

$$\pi(x_{k+1}|y_{1:k}) = \int \pi(x_{k+1}|x_k)\pi(x_k|y_{1:k})\,\mathrm{d}x_k, \tag{10}$$

where $\pi(y_k|y_{1:k-1}) = \int \pi(y_k|x_k)\pi(x_k|y_{1:k-1})\,\mathrm{d}x_k$. Equation (9) is the well-known Bayes theorem for conditional probability, and it computes the posterior (filtering) density $\pi(x_k|y_{1:k})$ as the product of the prior density $\pi(x_k|y_{1:k-1})$ and the likelihood function $\pi(y_k|x_k)$ divided by the normalization constant $\pi(y_k|y_{1:k-1})$; equation (10) is the well-known Chapman–Kolmogorov equation, which allows computing the next prior density exploiting knowledge of the transition kernel $\pi(x_{k+1}|x_k)$. Given the density of the initial state $\pi(x_1)$ and appropriate models for the likelihood and the transition kernel, the two previous equations sequentially compute the Bayesian solution for all the time samples.

3.1. Kalman filter

The framework of Bayesian filtering is quite general, in the sense that no assumptions are made on the shape of the probability densities, nor on the linearity of the model or of the state evolution. In this subsection we consider the class of linear Gaussian problems, i.e., the problems where the model equations are

$$Y_k = G_k \cdot X_k + N_k \tag{11}$$

$$X_{k+1} = F_k \cdot X_k + \Delta X_k, \tag{12}$$

where G_k, F_k are known matrices and X_0, N_k and ΔX_k are independent with Gaussian distributions. In this case, it can be proved [10] that all the prior and posterior densities are Gaussian; the application of equations (9), (10) only involves updating the mean and the covariance matrix of these Gaussian densities and analytic formulae are available: if we denote by $\bar{x}_{k|k-1}$ and $\Gamma_{k|k-1}$ the mean and the covariance of the prior density, and by $\bar{x}_{k|k}$ and $\Gamma_{k|k}$ the mean and the covariance of the posterior density, the recursive application of the following equations provide the solution of the Bayesian filtering:

$$\bar{x}_{k|k} = \bar{x}_{k|k-1} + K_k(y_k - G_k\bar{x}_{k|k-1}) \tag{13}$$

$$\Gamma_{k|k} = (1 - K_k G_k)\Gamma_{k|k-1} \tag{14}$$

$$\bar{x}_{k+1|k} = F_k\bar{x}_{k|k} \tag{15}$$

$$\Gamma_{k+1|k} = F_k\Gamma_{k|k}F_k^T + \Psi_k \tag{16}$$

$$K_k = \Gamma_{k|k-1}G_k^T\left(G_k\Gamma_{k|k-1}G_k^T + \Sigma_k\right)^{-1}, \tag{17}$$

where Ψ_k is the covariance matrix associated with ΔX_k and Σ_k is the covariance matrix associated with N_k. The previous set of equations is known as Kalman filter and provides the analytic computation of the Bayesian filtering equations when the restrictive assumptions are fulfilled. Clearly, in this case no algorithm can do better than the Kalman filter.

3.2. Particle filters

For nonlinear problems or non-Gaussian densities, the computation of equations (9), (10) requires the use of numerical approximation techniques. In the case of mildly nonlinear problems, one can use a local linearization of the model equations; the resulting algorithm is known as extended Kalman filter. When such a local linearization is not feasible, it is possible to use Monte Carlo approximation methods: in Monte Carlo integration, a density $\pi(x)$ is represented by a set of weighted points, where the points x^l and the weights w^l are determined by the density itself in such a way that for any integrable function f the following holds:

$$\sum_{l=1}^{N} w^l f(x^l) \overset{N\to\infty}{\longrightarrow} \int f(x)\pi(x)\,\mathrm{d}x, \tag{18}$$

which can also be interpreted as the approximation of the density

$$\pi(x) \simeq \sum_{l=1}^{N} w^l \delta(x - x^l). \tag{19}$$

In particular, if one is able to obtain N independent, identically distributed (i.i.d.) random samples from $\pi(x)$ itself, then the law of large numbers guarantees that

$$\sum_{l=1}^{N} \frac{1}{N} f(x^l) \overset{N\to\infty}{\longrightarrow} \int f(x)\pi(x)\,\mathrm{d}x. \tag{20}$$

When sampling directly from the density $\pi(x)$ is not possible, one can use an importance sampling strategy which consists of drawing N points x_q^l according to a so-called proposal, or importance, density $q(x)$; the proposal density is required to be nonzero where the density $\pi(x)$ is nonzero, and to be easy to sample from. Then the non-uniform weights

$$w^l = w\left(x_q^l\right) = \frac{\pi\left(x_q^l\right)}{q\left(x_q^l\right)} \tag{21}$$

are assigned to these points and the convergence (18) is still guaranteed by the law of large numbers.

Particle filters [1] are a class of algorithms which adopt a sequential importance sampling strategy for systematically solving the Bayesian filtering problem (9), (10): at each time sample, N particles x_k^l are drawn from a proposal density $q(x_k|y_{1:k-1})$, and the corresponding weights

$$w_k^l = \frac{\pi\left(x_k^l|y_{1:k}\right)}{q\left(x_k^l|y_{1:k-1}\right)} \tag{22}$$

are computed. In the simplest case, one can use the prior density $\pi(x_k|y_{1:k-1})$ as proposal density. With this choice, the Bayes theorem (9) implies that the computation of the weights reduces to the computation of the likelihood function: in fact, the weights are always determined up to a normalizing constant, and the denominator of equation (9) needs not to be computed; furthermore, the importance density itself can be evaluated through the use of the Chapman–Kolmogorov equation. Therefore the main steps of the most widely used particle filter, which is known as sampling importance resampling (SIR) filter or bootstrap filter are:

(Step 0) initialization: set an initial prior density which is easy to sample from, $\pi(x_1|\emptyset)$, and draw N particles; then for $k = 1, \ldots$.

(Step 1) filtering: apply Bayes theorem through the importance sampling procedure: assign the importance weights $w_k^l = \pi\left(y_k|x_k^l\right)$ to get the following approximation of the filtering density:

$$\pi(x_k|y_{1:k}) \simeq \sum_{l=1}^{N} w_k^l \delta\left(x_k - x_k^l\right). \tag{23}$$

(Step 2) resampling: after the filtering step, and depending on the width of the likelihood function and of the prior density, it may happen that most particles get a negligible weight; therefore the approximated filtering density $\sum_{l=1}^{N} w_k^l \delta\left(x_k - x_k^l\right)$ is randomly sampled in order to obtain the new approximation $\sum_{l=1}^{N}(1/N)\delta\left(x_k - \tilde{x}_k^l\right)$: the set $\left\{\tilde{x}_k^l\right\}_{l=1}^{N}$ of the new particles is a subset of $\left\{x_k^l\right\}_{l=1}^{N}$, where particles x_k^l corresponding to large weights w_k^l are drawn many times.

(Step 3) prediction: replace $\pi(x_k|y_{1:k})$ in the Chapman–Kolmogorov equation (10) with $\sum_{l=1}^{N}(1/N)\delta\left(x_k - \tilde{x}_k^l\right)$ to obtain

$$\pi(x_{k+1}|y_{1:k}) \simeq \frac{1}{N}\sum_{l=1}^{N} \pi\left(x_{k+1}|\tilde{x}_k^l\right) \tag{24}$$

and extract N new particles from this new prior. Technically, in our implementation this is done by extracting one random point from each $\pi\left(x_{k+1}\middle|\tilde{x}_k^l\right)$. Another possibility, leading to comparable results, would be to extract independent samples from the whole mixture.

Remark 3.1. The resampling step introduces correlation among the particles, so that convergence results, which are straightforward for the importance sampling, become here more problematic but still hold under some additional assumption [4].

Remark 3.2. Once the posterior density has been sampled by the filter, the solution can be estimated in different ways. In this paper, we will use particle and weights to compute the conditional mean of the solution.

4. Rao–Blackwellization

Let us now formulate the MEG inverse problem within the Bayesian filtering framework. The unknown is represented by the time-discrete stochastic process $\{\mathbf{J}_k\}_{k=1}^T$, where each random variable $\mathbf{J}_k$ is the pair of random variable $\mathbf{R}_k$, denoting the source position, and $\mathbf{Q}_k$, denoting the source amplitude. The data are represented by the time-discrete stochastic process $\{\mathbf{B}_k\}_{k=1}^T$ and each realization $\mathbf{b}_k$ is the measured biomagnetic field at time t_k. From the Biot–Savart equation (1) the model for the stochastic processes in the case of a single source (the generalization to multiple sources is straightforward) is given by

$$\mathbf{B}_k = G(\mathbf{R}_k)\mathbf{Q}_k + \mathbf{N}_k, \tag{25}$$

where, at a given sensor location $\mathbf{r}$ outside the skull,

$$G(\mathbf{R}_k) = \frac{\mu_0}{4\pi f^2}\mathbf{R}_k \times (f\mathbf{e}(\mathbf{r}) - \nabla f \cdot \mathbf{e}(\mathbf{r})\mathbf{r}) \tag{26}$$

is obtained from (3) using the canonical recursive properties of the inner and outer products in $\mathbb{R}^3$; here, $\mathbf{e}(\mathbf{r})$ represents the unit vector orthogonal to the sensor surface. We assume that the evolution of the system is described by equations

$$\mathbf{R}_{k+1} = \mathbf{R}_k + \Delta\mathbf{R}_k, \tag{27}$$

$$\mathbf{Q}_{k+1} = \mathbf{Q}_k + \Delta\mathbf{Q}_k, \tag{28}$$

where $\Delta\mathbf{R}_k$ and $\Delta\mathbf{Q}_k$ are assumed to be Gaussian. Under Markovian assumptions analogous to (6)–(8), Bayesian filtering can be applied to track the stochastic process $\{\mathbf{J}_k\}_{k=1}^N$, where the posterior probability density function can be computed by applying a standard SIR particle filter. We point out that describing the temporal dynamics in the brain by means of a random walk as in (27) means that a small amount of *a priori* information on the temporal evolution is introduced in the model. In fact, utilizing more realistic transition kernels would correspond to introducing more featured, less general priors (see equation (10)).

We remark in equation (25) that the dependence of the measured variable $\mathbf{B}_k$ on the dipole amplitude $\mathbf{Q}_k$ is linear. Therefore, if $\mathbf{N}_k$ and $\Delta\mathbf{Q}_k$ are Gaussian variables, even $\mathbf{Q}_k$ is Gaussian and its moments can be analytically determined by applying a Kalman filter. In terms of probability density functions, the factorization

$$\pi(\mathbf{j}_k|\mathbf{b}_{1:k}) = \pi(\mathbf{q}_k|\mathbf{r}_k, \mathbf{b}_{1:k})\pi(\mathbf{r}_k|\mathbf{b}_{1:k}) \tag{29}$$

holds and the Gaussian function $\pi(\mathbf{q}_k|\mathbf{r}_k, \mathbf{b}_{1:k})$ is analytically computed by using the set of equations (13)–(17). Furthermore, under the Markovian properties

$$\pi(\mathbf{r}_k|\mathbf{r}_{1:k-1}) = \pi(\mathbf{r}_k|\mathbf{r}_{k-1}), \tag{30}$$

$$\pi(\mathbf{b}_k|\mathbf{r}_{1:k}) = \pi(\mathbf{b}_k|\mathbf{r}_k) \tag{31}$$

and

$$\pi(\mathbf{r}_{k+1}|\mathbf{r}_k, \mathbf{b}_{1:k}) = \pi(\mathbf{r}_{k+1}|\mathbf{r}_k) \tag{32}$$

concerned with the stochastic process $\{\mathbf{R}_k\}_{k=1}^T$, a new SIR particle filter allows the computation of the posterior $\pi(\mathbf{r}_k|\mathbf{b}_{1:k})$ within the usual Bayesian filtering framework. However, in this case, the measurements are no longer independent when conditioned on the particles:

Theorem 4.1. *If* $\mathbf{Q}_0$, $\mathbf{N}_k$ *and* $\Delta\mathbf{Q}_k$ *are Gaussian variables,* $\mathbf{N}_k$ *has zero mean and* $\pi(\mathbf{r}_k|\mathbf{b}_{1:k-1})$ *is used as proposal density for the importance sampling of* $\pi(\mathbf{r}_k|\mathbf{b}_{1:k})$*, then the weights of the corresponding SIR particle filter are*

$$w_{R_k}^l = \frac{\pi\left(\mathbf{b}_k\middle|\mathbf{r}_k^l, \mathbf{b}_{1:k-1}\right)}{\pi(\mathbf{b}_k|\mathbf{b}_{1:k-1})}; \tag{33}$$

$\pi(\mathbf{b}_k|\mathbf{r}_k, \mathbf{b}_{1:k-1})$ *is a Gaussian function with mean value*

$$\mathbf{b}_k^l = G\left(\mathbf{r}_k^l\right) E\left(\mathbf{Q}_k|\mathbf{r}_k^l, \mathbf{b}_{1:k-1}\right) \tag{34}$$

and covariance

$$\mathbf{C}_k^l = G\left(\mathbf{r}_k^l\right)\Gamma_k^l G\left(\mathbf{r}_k^l\right)^T + \Sigma_k, \tag{35}$$

where

$$\begin{aligned}\Gamma_k^l &= E\left(\left(\mathbf{Q}_k - \mathbf{q}_k^l\right)\left(\mathbf{Q}_k - \mathbf{q}_k^l\right)^T\middle|\mathbf{r}_k^l, \mathbf{b}_{1:k-1}\right)\\ &= \int \left(\mathbf{q}_k - \mathbf{q}_k^l\right)\left(\mathbf{q}_k - \mathbf{q}_k^l\right)^\top \pi\left(\mathbf{q}_k\middle|\mathbf{r}_k^l, \mathbf{b}_{1:k-1}\right) \mathrm{d}\mathbf{q}_k\end{aligned} \tag{36}$$

and

$$\mathbf{q}_k^l = E\left(\mathbf{Q}_k\middle|\mathbf{r}_k^l, \mathbf{b}_{1:k-1}\right) = \int \mathbf{q}_k \pi\left(\mathbf{q}_k\middle|\mathbf{r}_k^l, \mathbf{b}_{1:k-1}\right) \mathrm{d}\mathbf{q}_k. \tag{37}$$

Proof. Model (25) implies

$$\begin{aligned}\mathbf{B}_k\left|\mathbf{r}_k^l, \mathbf{b}_{1:k-1}\right. &= G\left(\mathbf{r}_k^l\right) \cdot \mathbf{Q}_k\left|\mathbf{r}_k^l, \mathbf{b}_{1:k-1}\right. + \mathbf{N}_k\left|\mathbf{r}_k^l, \mathbf{b}_{1:k-1}\right.\\ &= G\left(\mathbf{r}_k^l\right) \cdot \mathbf{Q}_k\left|\mathbf{r}_k^l, \mathbf{b}_{1:k-1}\right. + \mathbf{N}_k.\end{aligned} \tag{38}$$

Therefore $\mathbf{B}_k\left|\mathbf{r}_k^l, \mathbf{b}_{1:k-1}\right.$ is the sum of two Gaussian random variables and is a Gaussian variable itself. Formulae (34)–(37) come by a straightforward computation from the definition of mean value and covariance. □

Remark 4.2. In the previous theorem the rather obvious notation $\mathbf{Q}_k\left|\mathbf{r}_k^l, \mathbf{b}_{1:k-1}\right.$ denotes the stochastic variable representing the dipole amplitude at time step k conditioned on the realizations $\mathbf{r}_k^l$ and $\mathbf{b}_{1:k-1}$ (an analogous meaning holds for the other conditioned variables in the theorem). Therefore $E\left(\mathbf{Q}_k\left|\mathbf{r}_k^l, \mathbf{b}_{1:k-1}\right.\right)$ and Γ_k^l are the mean value and variance provided by the Kalman filter.

In the present context, Rao–Blackwellization is the procedure that consists in assessing the posterior distribution $\pi(\mathbf{j}_k|\mathbf{b}_{1:k})$ as the product of the estimates of $\pi(\mathbf{q}_k|\mathbf{r}_k, \mathbf{b}_{1:k})$ times $\pi(\mathbf{r}_k|\mathbf{b}_{1:k})$ where $\pi(\mathbf{q}_k|\mathbf{r}_k, \mathbf{b}_{1:k})$ is optimally determined by applying a set of Kalman filters and $\pi(\mathbf{r}_k|\mathbf{b}_{1:k})$ is sampled by means of a particle filter. When applicable, a Rao–Blackwellized particle filter should be preferred to a standard particle filter for essentially three computational reasons. First, the Kalman filter optimally computes $\pi(\mathbf{q}_k|\mathbf{r}_k, \mathbf{b}_{1:k})$ without the need of any sampling. Second, if M is the number of active sources, a particle filter for $\pi(\mathbf{r}_k|\mathbf{b}_{1:k})$ samples

particles in $\mathbb{R}^{3M}$ while a particle for $\pi(\mathbf{j}_k|\mathbf{b}_{1:k})$ samples particles in $\mathbb{R}^{6M}$. Third, as proved in the following theorem, the variance of the weights in the particle filter for $\pi(\mathbf{r}_k|\mathbf{b}_{1:k})$ is smaller than the variance of the weights in the particle filter for $\pi(\mathbf{j}_k|\mathbf{b}_{1:k})$, i.e. the sampling of $\pi(\mathbf{r}_k|\mathbf{b}_{1:k})$ is more efficient. In the following theorem, we use the notation $E_{\pi(x)}(f(x)) := \int f(x)\pi(x)\,\mathrm{d}x$ and $\mathrm{var}_{\pi(x)}(f(x)) := \int (f(x) - E_{\pi(x)}(f(x)))^2\pi(x)\,\mathrm{d}x$, with the obvious generalization to random vectors.

Theorem 4.3. *[5] Given the two random variables*

$$w(\mathbf{J}_k) = \frac{\pi(\mathbf{J}_k|\mathbf{b}_{1:k})}{\pi(\mathbf{J}_k|\mathbf{b}_{1:k-1})} \tag{39}$$

and

$$w(\mathbf{R}_k) = \frac{\pi(\mathbf{R}_k|\mathbf{b}_{1:k})}{\pi(\mathbf{R}_k|\mathbf{b}_{1:k-1})}, \tag{40}$$

then

$$\mathrm{var}_{\pi(\mathbf{j}_k|\mathbf{b}_{1:k-1})}(w(\mathbf{J}_k)) \geqslant \mathrm{var}_{\pi(\mathbf{r}_k|\mathbf{b}_{1:k-1})}(w(\mathbf{R}_k)). \tag{41}$$

Proof. We first observe that

$$w(\mathbf{R}_k) = E_{\pi(\mathbf{q}_k|\mathbf{r}_k,\mathbf{b}_{1:k-1})}(w(\mathbf{J}_k)). \tag{42}$$

Therefore

$$\begin{aligned}\mathrm{var}_{\pi(\mathbf{r}_k|\mathbf{b}_{1:k-1})}(w(\mathbf{R}_k)) &= E_{\pi(\mathbf{r}_k|\mathbf{b}_{1:k-1})}(E_{\pi(\mathbf{q}_k|\mathbf{r}_k,\mathbf{b}_{1:k-1})}(w(\mathbf{J}_k))^2) \\ &\quad - (E_{\pi(\mathbf{r}_k|\mathbf{b}_{1:k-1})}(E_{\pi(\mathbf{q}_k|\mathbf{r}_k,\mathbf{b}_{1:k-1})}(w(\mathbf{J}_k))))^2 \\ &= E_{\pi(\mathbf{r}_k|\mathbf{b}_{1:k-1})}(E_{\pi(\mathbf{q}_k|\mathbf{r}_k,\mathbf{b}_{1:k-1})}(w(\mathbf{J}_k))^2) - (E_{\pi(\mathbf{j}_k|\mathbf{b}_{1:k-1})}(w(\mathbf{J}_k)))^2. \end{aligned} \tag{43}$$

Now we subtract (43) to

$$\mathrm{var}_{\pi(\mathbf{j}_k|\mathbf{b}_{1:k-1})}(w(\mathbf{J}_k)) = E_{\pi(\mathbf{j}_k|\mathbf{b}_{1:k-1})}(w(\mathbf{J}_k)^2) - (E_{\pi(\mathbf{j}_k|\mathbf{b}_{1:k-1})}(w(\mathbf{J}_k)))^2 \tag{44}$$

and obtain

$$\begin{aligned}&\mathrm{var}_{\pi(\mathbf{j}_k|\mathbf{b}_{1:k-1})}(w(\mathbf{J}_k)) - \mathrm{var}_{\pi(\mathbf{r}_k|\mathbf{b}_{1:k-1})}(w(\mathbf{R}_k)) \\ &\qquad = E_{\pi(\mathbf{r}_k|\mathbf{b}_{1:k-1})}(\mathrm{var}_{\pi(\mathbf{q}_k|\mathbf{r}_k,\mathbf{b}_{1:k-1})}(w(\mathbf{J}_k))), \end{aligned} \tag{45}$$

where the term at the right-hand side is positive. □

Starting from the previous theoretical considerations the Rao–Blackwellized particle filter algorithm we have implemented consists of the following steps:

(Step 0) initialization: set an initial prior density which is easy to sample from, $\pi(\mathbf{r}_1|\emptyset)$, and draw N particles; then, for $k = 1, \ldots$.

(Step 1) filtering—Kalman filter: for each particle $\mathbf{r}_k^l$ update the mean and the covariance of the linear variable $\mathbf{Q_k}$ by means of equations (13), (14) and (17).

(Step 2) filtering—particle filter: apply Bayes theorem through the importance sampling procedure: assign the importance weights $w_k^l = \pi\left(\mathbf{b}_k\middle|\mathbf{r}_k^l, \mathbf{b}_{1:k-1}\right)$ to get the approximation of the filtering density.

(Step 3) resampling: the usual resampling step for SIR particle filtering.

(Step 4) prediction—Kalman filter: for each particle $\mathbf{r}_k^l$ update the mean and the covariance of the linear variable $\mathbf{Q_k}$ by means of equations (15) and (16).

(Step 5) prediction—particle filter: the usual prediction step for SIR particle filtering.

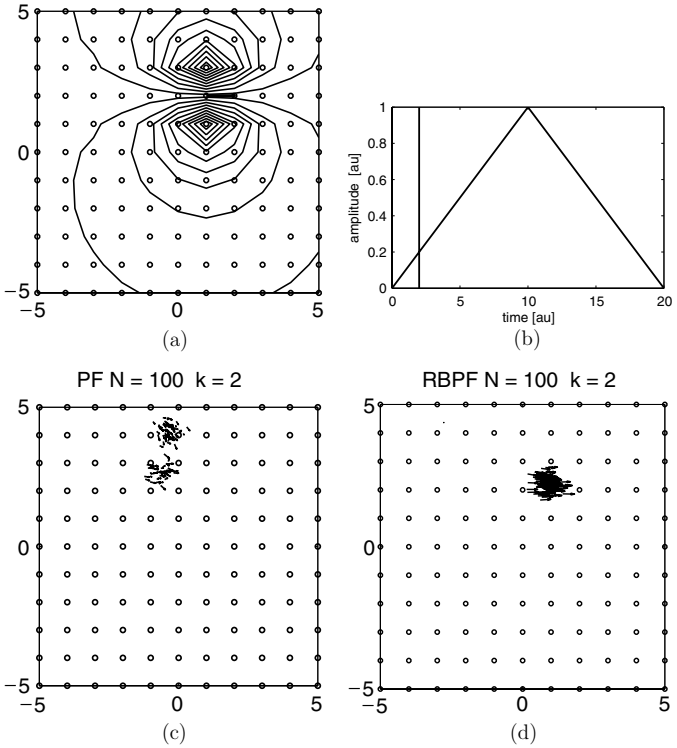

Figure 1. The magnetic field (a) produced by the dipole with amplitude in (b). The particle filter approximation of the posterior density reconstructed with PF (c) and RBPF (d) at the second time point.

5. Numerical applications

A preliminary comparison between the computational costs of a particle filter (PF in this section) and a Rao–Blackwellized particle filter (RBPF in this section) should account for the following two issues: first, RBPF samples $\pi(\mathbf{r}_k|\mathbf{b}_{1:k})$ instead of $\pi(\mathbf{j}_k|\mathbf{b}_{1:k})$, which implies that the computational time for the sampling procedure is essentially halved. Second, in RBPF, a not-negligible contribution to the overall computational cost comes from the execution of the Kalman filter. In order to actually assess the real gain provided by Rao–Blackwellization we consider some applications involving both real and simulated data realized with a high-performances desktop PC.

Simulated data are computed by inserting a current dipole distribution into equation (3) and by affecting the resulting magnetic time series with Gaussian noise of notable intensity, so that the signal-to-noise ratio is close to the one of typical averaged biomagnetic data in MEG real experiments. Both the prior pdf and the transition kernel are chosen to be Gaussian distribution.

As a first synthetic case, in figure 1 we apply the two filters in a very easy two-dimensional situation, where the magnetic field in figure 1(a) is produced by the current dipole with time behavior in figure 1(b). Figures 1(c) and (d) show the particle distributions at the time point highlighted in figure 1(b). In both reconstructions we used $N = 100$ particles: in this situation PF provides its reconstruction at each time point in 1.75 s while for RBPF the time for a single time sample increases up to 2.15 s. However the Rao–Blackwellized algorithm correctly

Table 1. Averaged reconstruction errors on the position (in cm) and on the orientation (in rad) and averaged root-mean-squares errors for the amplitude reconstruction given by PF (with 50 000 particles) and RBPF (with 1000 particles) in the case of figure 2.

	Position (cm)	Orientation (rad)	Amplitude
Dipole A PF	0.8	0.064	15.0%
Dipole A RBPF	0.45	0.051	8.8%
Dipole B PF	1.13	0.16	31.0%
Dipole B RBPF	0.81	0.15	18.1 %

recovers the source already at the second time point, when the particle distribution provided by the particle filter is still far from correctly localizing the source. This implies that 100 particles are certainly insufficient for PF to provide an accurate reconstruction of the source dipole.

To better show this difference in accuracy performances, we consider a more realistic experiment where, in a three-dimensional geometry, two current dipoles located in completely different positions in the brain are characterized by overlapping amplitudes. These amplitudes are represented in figure 2(a) while the original location of the dipoles is in figure 2(b). Figures 2(c) and (d) present the conditional mean at different time points: the reconstruction in (c) has been obtained with the particle filter code employing $N = 50\,000$ particles while Rao–Blackwellization allows one to obtain the better result in (d) with a notably reduced number of input particles ($N = 1000$). Figures 2(e) and (f) show the reconstructions of the amplitudes provided by PF and RBPF. We notice that PF provides the whole reconstruction in 6000 s per time sample while for RBPF the computational time is 154.5 s per time sample. Furthermore, in table 1, we describe more quantitatively the reliability of these reconstructions providing the reconstruction error on the position (given as the distance in centimeter between the true and restored dipoles' positions averaged over the time interval and over ten runs of the algorithm), the reconstruction error on the orientation (given as the difference in radian between the true and restored dipoles' orientations averaged over the time interval and over ten runs of the algorithm) and the reconstruction error on the amplitude (given as the root-mean-square error averaged over ten runs of the algorithm). The table shows that RBPF is always more accurate than PF.

Figure 3 contains another quantitative assessment of the differences between the performances of the two algorithms. In the first row we analyze the biomagnetic data produced by a single dipole (dipole A in the example of figure 2) with PF and the RBPF with the same number $N = 100$ of input particles and in figures 3(a) and (b) compute the reconstruction error on the position and on the orientation. In figure 3(c) we also superimpose the theoretical amplitude on the amplitudes reconstructed by the two algorithms. These plots show that in the case of a very small number of particles Rao–Blackwellization allows a notable improvement of the reconstruction accuracy. Figures 3(d)–(f) contain the same information as in (a)–(c) respectively, but this time with $N = 1000$ particles in the case of the particle filter algorithm. These results show that Rao–Blackwellization allows a reduction of 90% in the number of input particles without deteriorating the reconstruction accuracy.

Finally, in figure 4 we compare the performances of the two algorithms in the case of a real data set recorded with a 306-channel whole-head neuromagnetometer (Elekta Neuromag Oy, Helsinki, Finland), which employs 102 sensor elements, each comprising one magnetometer and two planar gradiometers. Measurements were filtered in the range 0.1–170 Hz and sampled at 600 Hz. Prior to the actual recording, four small indicator coils attached to the scalp at locations known with respect to anatomical landmarks were energized and the elicited

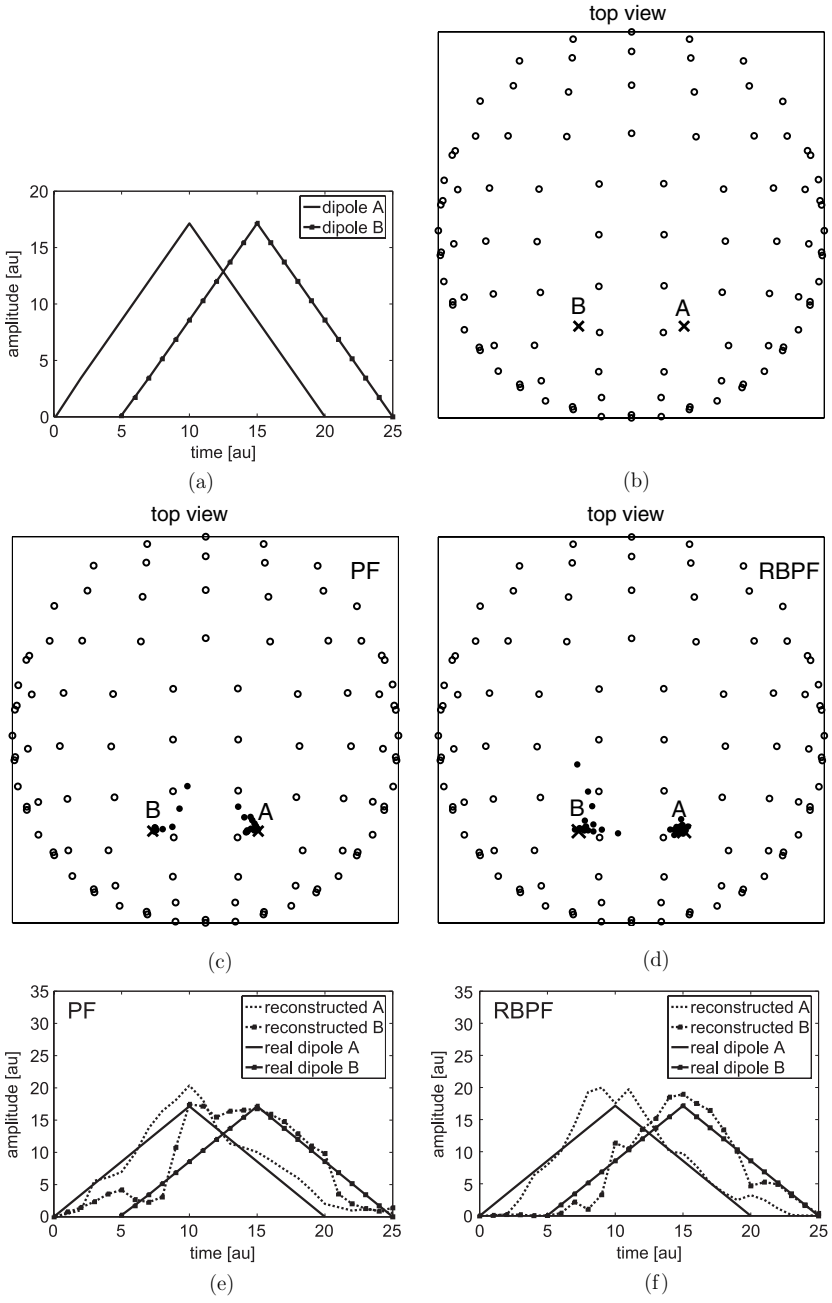

Figure 2. Amplitudes (a) and positions (b) of the original dipoles. Conditional mean of the posterior density obtained with PF (c) and RBPF (d) at different time points. Reconstructed amplitudes obtained with PF (e) and RBPF (f). PF utilizes $N = 50\,000$ particles while for RBPF $N = 1000$.

magnetic fields recorded to localize the head with respect to the MEG sensors and thus to allow subsequent co-registration of the MEG with anatomical MR-images. Epochs with exceedingly large ($b > 3$ pT = cm) MEG signal excursions were rejected, and about 100 artifact-free trials

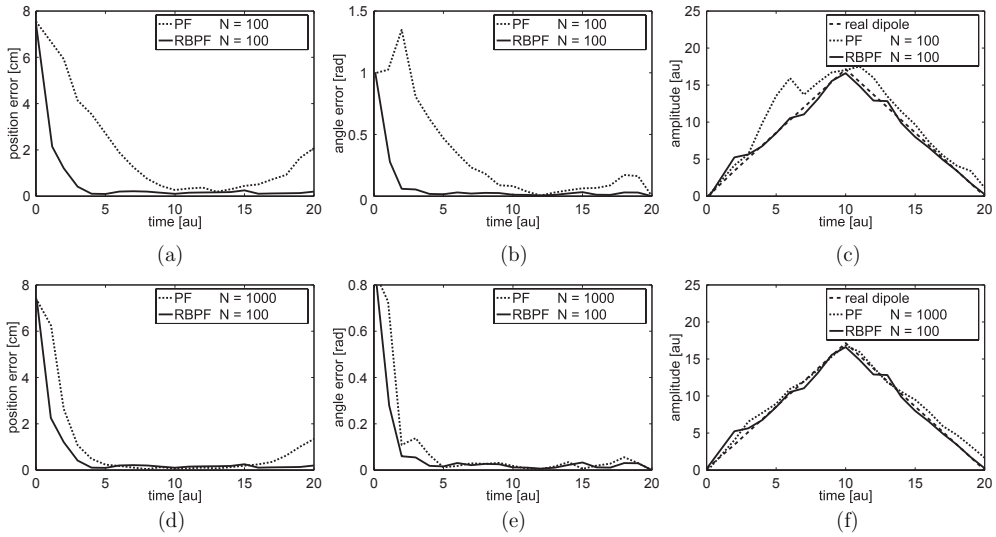

Figure 3. Reconstruction of the dipole A in figure 2(a): position error (a), orientation error (b) and reconstructed amplitude (c) obtained using 100 particles for both the algorithms. The same objects (respectively (d)–(f)) with 100 particles for RBPF and 1000 for PF.

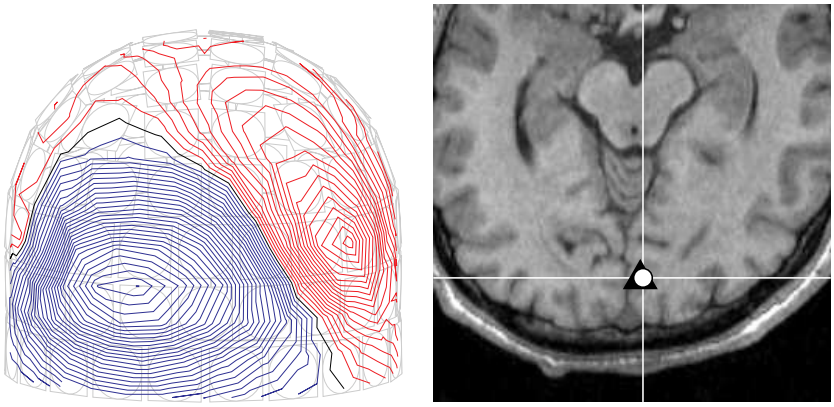

Figure 4. A real experiment with visual stimulation: (a) the measured magnetic field at the peak time point; (b) coregistration on a magnetic resonance high-resolution axial view of the sources reconstructed by PF and RBPF. The two reconstructed dipoles coincide but PF (triangle) employees $N = 50\,000$ particles while RBPF (circle) utilizes only $N = 1000$ particles.

(This figure is in colour only in the electronic version)

of each stimulus category were collected and averaged on-line in windows $[-100, 500]$ ms with respect to the stimulus onset. Residual environmental magnetic interference was subsequently removed from the averages using the signal–space separation method [19]. We considered a visual external stimulation. Figure 4(a) shows the magnetic field at the peak time point while figure 4(b) shows an axial view of the reconstructions provided by PF and RBPF: the two

reconstructions are essentially the same but again PF utilizes $N = 50\,000$ particles to obtain a stable dipole while for RBPF $N = 1000$ are surely enough.

6. Conclusions and open problems

In this paper, we have discussed the effectiveness of a Rao–Blackwellized particle filter in reconstructing neural sources from biomagnetic MEG data. We have shown that this approach is advantageous with respect to a standard SIR particle filter, inasmuch as it provides accurate reconstructions with a significantly lower computational effort. The typical neurophysiological conditions, particularly in the case of visual stimuli (see, for example, [18]) involve the activation of complex neural constellations and require the analysis of relatively long-time series. We think that a systematic application of a Bayesian filtering approach for the analysis of MEG data would be favored by the use of Rao–Blackwellization, and, in order to validate this conjecture, we are currently planning to systematically apply our RBPF to many real data sets acquired during visual stimulations of different degrees of complexity.

Finally, from a more computational viewpoint, we are working at a further reduction of the numerical heaviness of the analysis by introducing a computational grid where computing the Rao–Blackwellized filter.

References

[1] Arulampalam M S, Maskell S, Gordon N and Clapp T 2002 A tutorial on particle filters for online nonlinear/non-Gaussian Bayesian tracking IEEE *Trans. Signal Process.* **50** 174–88
[2] Cantarella J, De Turck D and Gluck H 2001 The Biot–Savart operator for application to knot theory, fluid dynamics, and plasma physics *J. Math. Phys.* **42** 876–905
[3] Casella G and Robert C P 1996 Rao–Blackwellisation of sampling schemes *Biometrika* **83** 81–94
[4] Doucet A, Godsill S and Andrieu C 2000 On sequential Monte Carlo sampling methods for Bayesian filtering *Stat. Comput.* **10** 197–208
[5] Doucet A, Gordon N J and Krishnamurthy V 2001 Particle filters for state estimation of jump Markov linear systems IEEE *Trans. Signal. Process.* **49** 613–24
[6] Gencer N V and Tanzer I O 1999 Forward problem solution of electromagnetic source imaging using a new BEM formulation with high-order elements *Phys. Med. Biol.* **44** 2275–87
[7] Hämäläinen M and Ilmoniemi R J 1994 Interpreting magnetic fields of the brain: minimum-norm estimates *Med. Biol. Eng. Comput.* **32** 35–42
[8] Hari R, Hämäläinen M, Knuutila J and Lounasmaa O V 1993 Magnetoencephalography: theory, instrumentation and applications to non-invasive studies of the working human brain *Rev. Mod. Phys.* **65** 2
[9] Hari R, Karhu J, Hämäläinen M, Knuutila J, Salonen O, Sams M and Vilkman V 1993 Functional organization of the human first and second somatosensory cortices: a neuromagnetic study *Eur. J. Neurosci.* **5** 724–34
[10] Kaipio J and Somersalo E 2004 *Statistical and Computational Inverse Problem* (Berlin: Springer)
[11] Kress R, Kuhn L and Potthast R 2002 Reconstruction of a current distribution from its magnetic field *Inverse Problems* **18** 1127–46
[12] Mosher J C and Leahy R M 1999 Source Localization Using Recursively Applied and Projected (RAP) MUSIC IEEE *Trans. Signal Process.* **47** 332–40
[13] Pascarella A, Sorrentino A, Piana M and Parkkonen L 2007 Particle filters and rap-music in meg source modeling: a comparison *New Frontiers in Biomagnetism* (International Congress Series) 1300 pp 161–4
[14] Sarvas J 1987 Basic mathematical and electromagnetic concepts of the biomagnetic inverse problem *Phys. Med. Biol.* **32** 11–22
[15] Sekihara K, Nagarajan S S, Poeppel D, Marantz A and Miyashita Y 2002 Application of an MEG eigenspace beamformer to reconstructing spatio-temporal activities of neural sources *Hum. Brain Mapp.* **15** 199–215
[16] Somersalo E, Voutilainen A and Kaipio J P 2003 Non-stationary magnetoencephalography by Bayesian filtering of dipole models *Inverse Problems* **19** 1047–63
[17] Sorrentino A, Parkkonen L and Piana M 2007 Particle filters: a new method for reconstructing multiple current dipoles from MEG data *New Frontiers in Biomagnetism* (International Congress Series) 1300 pp 173–6

[18] Sorrentino A, Parkkonen L, Piana M, Massone A M, Narici L, Carozzo S, Riani M and Sannita W G 2006 Modulation of brain and behavioural responses to cognitive visual stimuli with varying signal-to-noise ratio *Clin. Neurophys.* **117** 1098–105

[19] Taulu S, Kajola M and Simola J 2004 Suppression of interference and artifacts by the signal space separation method *Brain Topogr.* **16** 269–75

[20] Uutela K, Hämäläinen M and Somersalo E 1999 Visualization of magnetoencephalographic data using minimum current estimates *NeuroImage* **10** 173–80

[21] Van Veen B D, van Drongelen W, Yuchtman M and Suzuki A 1997 Localization of brain electrical activity via linearly constrained minimum variance spatial filtering IEEE *Trans. Biom. Eng.* **44** 867–80